International Journal of Nanoelectronics and Materials
IJNeaM
ISSN 1985-5761 | E-ISSN 2232-1535

Electrospun Nanofibers from Durian Rind-Derived Nanocellulose: Influence of Tween 20 and Tween 80 on Morphology and Structure for Livestock Semen Preservation

Azima Azmi[a,*], Ainaa Abdul Kahar[a], Nur Sabrina Wahab[a], Muhammad Zaidi Abu Bakar[a], Mariah Batrisyia Muhammad[b] Ainu Husna M S Suhaim[c], Julie Marzlinda Mohd Razak[c], Abdul Mu'in Hassan Basri[c], Shazwan Abd. Shukor[a], Nurul Hazwani Aminuddin Rosli[d], Chin Hua Chia[e,] and Shahariah Chowdhury[f]

[a]*Biotechnology & Nanotechnology Research Center, Malaysian Agricultural Research & Development Institute (MARDI), Persiaran MARDI-UPM, 43400 Serdang, Selangor, Malaysia*
[b]*Department of Biotechnology, IIUM Kuantan Campus, International Islamic University Malaysia, Jalan Sultan Haji Ahmad Shah, Bandar Indera Mahkota, 25200 Kuantan, Pahang Darul Makmur, Malaysia*
[c]*Livestock Science Research Center, Malaysian Agricultural Research & Development Institute (MARDI), Persiaran MARDI-UPM, 43400 Serdang, Selangor, Malaysia*
[d]*Physics Department, Center for Defense Foundation Studies, Universiti Pertahanan Nasional Malaysia, 57000 Kuala Lumpur, Malaysia*
[e]*Materials Science Program, Faculty of Science and Technology, Universiti Kebangsaan Malaysia, 43600 Bangi, Selangor, Malaysia*
[f]*Health and Environmental Research Center, Faculty of Environmental Management, Prince of Songkla University, Hat Yai, Songkhla 90110, Thailand*
**Corresponding author. Tel.: +6-03-89536093; fax: +6-03-89536154; e-mail: azima@mardi.gov.my*

Received 29 June 2025, Revised 21 Feb 2026, Accepted 21 May 2026

ABSTRACT

This study explores the utilization of nanocellulose derived from durian rind as a reinforcing agent in electrospun nanofibers intended for potential use in livestock semen preservation. Nanocellulose was extracted through alkaline treatment followed by acid hydrolysis and incorporated into polyvinyl alcohol (PVA) solutions. Tween 20 and Tween 80 are selected to investigate the effect of dispersion and morphology on nanocellulose during the electrospinning process. FESEM, XRD, and FTIR were then used to characterize the electrospun nanofibers. Morphological images show that the electrospun nanofibers with Tween 80 are mostly uniform in width and surface appearance compared to those with Tween 20. Good fiber dispersion indicates that Tween 80 offers greater solution stability than Tween 20. FTIR spectra confirmed matrix bonding between polyvinyl alcohol (PVA) and nanocellulose, as well as the functional groups of both. X-ray diffraction (XRD) analysis indicated that electrospun nanofibers loaded with Tween 80 showed an elevated degree of crystallinity. This indicates the stability of the superior alignment structure. The enhanced characteristics observed in the electrospun nanofibers incorporated with Tween 80 suggest physical stability and significant barrier properties, which are key requirements for semen preservation applications. This study has demonstrated the viability of transforming agricultural by-products into valuable nanomaterials and highlighted the importance of selecting a suitable surfactant to modulate the properties of electrospun nanofibers. The data from this study show that electrospun nanofiber membranes could be promising, offering an alternative biocompatible material for semen preservation.

Keywords: *Nanocellulose, durian rind, semen preservation, surfactant*

1. INTRODUCTION

The preservation of livestock semen plays a crucial role in animal reproduction and genetic improvement programs. Cryopreservation is a common practice globally, but it has several disadvantages. The cryo-induced process can damage sperm cells, resulting in reduced motility, membrane failure, and increased operating costs (Watson, 2000; Yoon et al., 2020). Due to these challenges, researchers are exploring alternative bio-preservation methods, such as gel-based protective coatings made from biocompatible materials. Encapsulation creates a protective microenvironment that helps maintain sperm viability, minimizes oxidative damage, and extends their lifespan without involving extreme cooling conditions (Saragusty & Arav, 2011)

Recently, there has been increasing attention from researchers to the encapsulation of spermatozoa in natural, biodegradable matrices that keep them viable even at room temperature. These matrices resemble the body's natural supportive tissues, which have a porous structure that allows the exchange of substances while providing strength. Electrospinning offers a promising method for producing polymeric nanofibers that serve as a scaffold for spermatozoa and possess desirable properties. In 2008, Xie et al. demonstrated that sperm remained viable when embedded in electrospun nanofibers. Later, Marei's 2021 study showed that these coatings gently protect sperm cells while gradually supplying essential nutrients. Prior research by Bhahardwaj & Kundu (2010) highlighted the versatility of electrospun nanofibers' applications, including drug delivery systems, tissue engineering, cell encapsulation, and wound healing. Their adaptability

suggests that this electrospun nanofiber could serve various biological functions beyond sperm preservation. Researchers have demonstrated that encapsulating sperm with electrospun nanofibers safeguards sperm at room temperature, eliminating the need for refrigeration (Shariatpanah et al., 2022). In recent years, researchers have turned to natural, sustainable sources to produce electrospun nanofibers using eco-friendly methods. Agricultural waste, such as durian rind (Durio zibethinus), which accounts for about 60-70% of the fruit's weight and is frequently discarded, has emerged as a promising candidate, offering a sustainable, renewable resource. Hence, improper disposal of organic waste can lead to environmental concerns (Widya et al., 2020).

Furthermore, durian rind is abundant in lignocellulose, making it a suitable alternative source for electrospinning processes (Chinet et al., 2018; Shamsudin et al., 2019). Utilizing durian waste aligns with green chemistry principles, promotes a circular economy, adds value to farm byproducts, and reduces dependence on petroleum-based polymers. The cellulose derived from durian rind is biodegradable, biocompatible, and environmentally friendly, making it a promising material for gamete storage and other biomedical applications.

Adding tween 20 and tween 80 to the electrospinning mixture could enhance the functional characteristics and manufacturability of electrospun nanofibers. This mixture noticeably alters texture, absorbency, and loading capacity. This non-ionic surfactant effectively enhances dispersion, diminishes surface tension, and optimizes the encapsulation of biological materials (Jee et al., 2016). According to Sieme et al. (2016), surfactants can improve membrane integrity and reduce environmental stress caused by cold shock during storage. The use of Tween 20 and Tween 80 in the pharmaceutical and biological sectors is widespread due to their high biocompatibility and low toxicity, which make them ideal for semen encapsulation systems. The mixture of cellulose nanofibers alongside surfactants may provide a non-cryogenic encapsulation as an alternative method for preserving spermatozoa viability.

This study examined the viability of electrospun nanofiber membranes derived from durian rind cellulose, in conjunction with Tween 20 and Tween 80, for encapsulating and storing ruminant semen at ambient temperature, and investigated the physicochemical characteristics of the resulting fibers and the impact of using Tween 20 and Tween 80. By leveraging agricultural waste and surfactant-assisted electrospinning, this work contributes to the development of sustainable, low-cost alternatives to conventional cryopreservation in reproductive biotechnology.

2. MATERIALS AND METHODS

2.1. Materials

Durian rind (*Durio zibethinus*) was sourced from local markets and thoroughly washed to remove residual pulp and dirt. Sodium chlorite, 80% (Acros Organics), glacial acetic acid, 95% (R&M Chemicals), polyvinyl alcohol (PVA), Tween 20, and Tween 80 were obtained from Sigma-Aldrich. Livestock semen (bovine) was collected from MARDI Kluang, a certified veterinary center, in accordance with ethical approval guidelines.

2.2. Extraction of Cellulose from Durian Rind

The cleaned durian rind was cut into small pieces, oven-dried at 60°C for 48 hours until it reached <10% moisture content, and ground into powder. The durian rind powder was rinsed a few times with distilled water to remove impurities present during processing. Delignification was performed using acid-chlorite bleaching six times, with a total of 1.125 g/g sodium chlorite and 1.25 g/g acetic acid. After treatment, the sample was washed several times with distilled water, as shown in Figure 1(b), before nanofibrillation, which was performed using a high-speed blender with 0.7 wt% NaCl added as a counterion. The resulting cellulose was washed, dried, and stored in a desiccator.

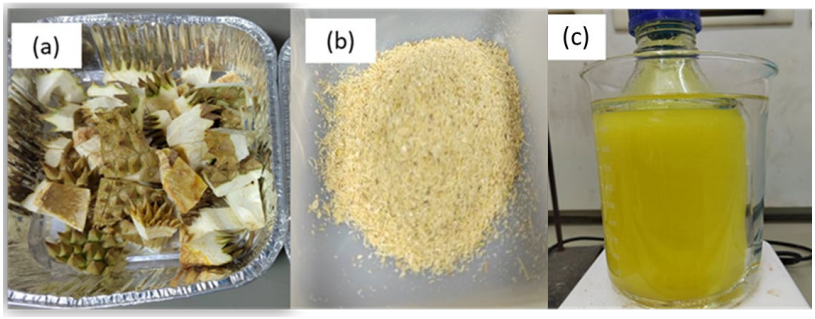

Figure 1. a) Cleaned durian rind (DR) cuts into small pieces, b) DR powder after oven-drying and grinding into powder, and c) delignification; acid chlorite bleaching process.

2.3. Preparation of Electrospinning Solution

The electrospinning solution was prepared by dissolving 15% (w/v) PVA in distilled water under constant stirring at 90°C until a clear solution was obtained. Extracted cellulose (1% w/v) was dispersed in the PVA solution under continuous stirring and sonication to ensure homogeneity. Tween 20 or Tween 80 was added at 1.0% (v/v) to the solution, and the mixture was promptly agitated to ensure homogeneity.

2.4. Electrospinning Process

The polymer solution was loaded into a 10 mL syringe fitted with a stainless-steel needle (21G) and electrospun using a high-voltage power supply. The optimized parameters for electrospinning were: voltage of 15–18 kV, flow rate of 0.8 mL/h, and a tip-to-collector distance of 15 cm. The nanofibers were collected on parchment paper for easy peel-off collection.

2.5. Characterization of Nanofibers

A square swatch of each cellulose membrane was observed under a field-emission microscope (FESEM, Hitachi SU8600). Electrospun nanofibers were also analysed by Fourier-transform infrared spectroscopy (FTIR, Perkin Elmer Spectrum 400) at a resolution of 1 cm^{-1} over the range of 4000–500 cm^{-1}; and using an X-ray diffractometer (Bruker XRD D8-Advance) with a monochromatic Cu Kα radiation source (λ = 0.1539 nm), a scan rate of 2°/min, and a 2θ scan range from 5° to 35° to detect the crystalline phase and structure of cellulose in the fiber. Diffraction peaks corresponded to the cellulose region. D spacing (d) according to Bragg's equation and the degree of crystallinity index (CrI%) of cellulose was calculated based on the equation below:

$$n\lambda = 2dsin\theta \quad [1]$$

where d is the interplanar spacing (D spacing), n is the order of diffraction, λ is a constant rate of 0.15406 nm, and θ is the peak position in radians.

$$CrI\% = \frac{Area\ of\ crystalline\ region}{Area\ of\ crystalline\ region + area\ of\ amorphous\ region} \times 100 \quad [2]$$

2.6. Semen Encapsulation

Freshly collected and stored semen was incorporated with polymer and mixed until uniform before being loaded into a 10 mL syringe to carry out the electrospinning process.

3. RESULTS AND DISCUSSION

To investigate the properties of the synthesized electrospun nanofibers, multiple investigations must be conducted, including assessments of the macroscopic appearance of durian rind cellulose nanofibrils (CNF) and the electrospun membranes. The characterization of the developed fibers was subsequently performed using FTIR, XRD, and FESEM.

3.1. Assessment of Macroscopic Appearance of Durian Rind Cellulose Nanofibrils and the Electrospun Membranes

Figure 2 illustrates the results of FESEM morphological pictures of nanocellulose obtained from durian rind. The images conclusively illustrated the successful synthesis of nanocellulose from durian rind, with an average size of 8.9-40 nm.

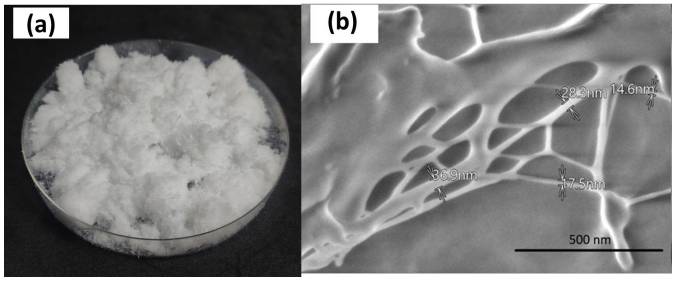

Figure 2. The images of (a) the production of CNF from durian rind and (b) the FESEM image for the morphology of the produced durian rind CNF.

Meanwhile, photographic images of the dried electrospun membranes are shown in Figure 3(a) PVA-Cellulose-Tween 20-Semen (PCTS-20) and Figure 3(b) PVA-Cellulose-Tween 80-Semen (PCTS-80). Both membranes exhibit flexible, translucent sheet-like morphology, but with observable differences in surface smoothness and structural integrity.
The sample in Figure 3(a) exhibits a more wrinkled surface at the edges, indicating weaker intermolecular interactions and mechanical cohesion. The inclusion of Tween 20, which has a shorter hydrophobic tail than Tween 80, could lead to reduced interfacial stabilization and diminished hydrogen bonding with the PVA-cellulose matrix. Discontinuities of this nature can diminish encapsulation efficiency, resulting in accelerated release or degradation in various application scenarios (Rezaei et al., 2020).

On the other hand, the sample in Figure 3(b) (PCTS-80) portrays a more uniform and cohesive membrane, suggesting improved molecular integration and film formation. The extended oleate chain present in Tween 80 may be a factor in this situation. The compatibility between PVA and CNF, both hydrophilic, with the biological material (semen) resulted in a more uniform matrix. Further studies showed that Tween 80 enhanced polymer miscibility and

plasticity, resulting in more uniform membranes (Zhou et al., 2015). From a macroscopic perspective, both membranes demonstrate flexibility and ease of peeling, which are essential for the actual handling and encapsulation of biological materials. Therefore, PCTS-80 is more suitable for encapsulations that require barrier stability, such as those used to prevent semen from breaking down, because it has fewer physical defects and a more uniform membrane.

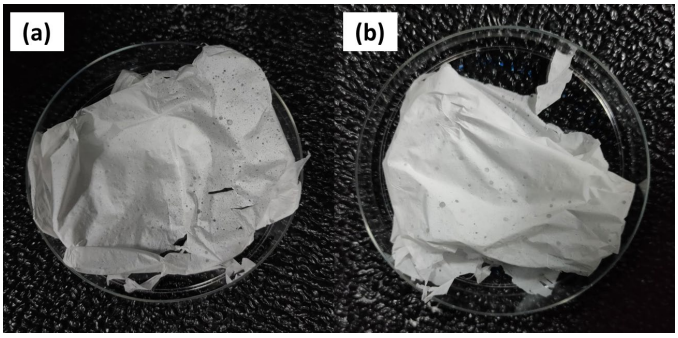

Figure 3. Macroscopic appearance of (a) PVA-Cellulose-Tween 20-semen (PCTS-20), (b) PVA-Cellulose-Tween 80-Semen (PCTS-80).

3.2. Fourier Transform Infrared (FTIR)

Nanocellulose, including cellulose nanofibrils (CNF), shows distinct FTIR peaks that can be attributed to the polysaccharide backbone. Electrospun nanofibers exhibit additional spectral features attributed to polymer mixing or chemical modification. This study compares the main FTIR peaks observed in nanocellulose with those in electrospun nanofibers, as shown in Figure 4.

The observation of a broad peak at 3324 cm-1 is attributed to hydrogen bonding and O-H stretching vibrations. This property of cellulose corresponds to the substantial intra and intermolecular hydrogen bonding among hydroxyl groups. The study of the nanocellulose peak indicates a sharp peak in contrast to the broader peak of cellulose, indicating a higher level of structural order (Rosa et al., 2010). The peak at 2914 cm^{-1} can be attributed to the symmetric and asymmetric stretching vibrations of the aliphatic C-H bond in the glucose ring. This is demonstrated by the existence of both nanocellulose and electrospun nanofiber spectra, as well as the response to the saturated hydrocarbon backbone of cellulose (Szyma-Chargot & Zdunek, 2013). The signal at 1732 cm^{-1} is attributed to the stretching of the carboxylic group (COOH. The peak is not observed in cellulose spectra. However, it is observed in electrospun nanofibers due to chemical modification induced by the incorporation of polyvinyl alcohol (PVA) and surfactants such as Tween 20 and Tween 80 (Li et al., 2009). The peak at 1634 cm^{-1} typically corresponds to the bending vibrations of water molecules (H-O-H) adsorbed within the hydrophilic nanocellulose matrix. The magnitude of this peak indicates the water content in the sample (Kargarzadech et al., 2012). The pronounced peak at 1029 cm-1 signifies the presence of C-O-C glycosidic linkages and C-O bonds in cellulose. Therefore, the fingerprint area validates the structure of the cellulose polysaccharide (Poletto et al., 2014). The peak near 834 cm^{-1} corresponds to the typical out-of-plane bending of the C-H bond, typically observed in aromatic rings or chains rather than in aliphatic polymers. However, this peak indicates a difference between the CNF and electrospun nanofiber bands, as it is absent in CNF due to the lack of structural features resulting from the mixing of PVA with surfactants such as Tween 80 and Tween 20. These additives introduce additional vibrational modes in the IR region around 830 cm^{-1} that are not intrinsic to the native cellulose structure. This proves the presence of surfactant Tween 80 in the electrospun nanofiber.

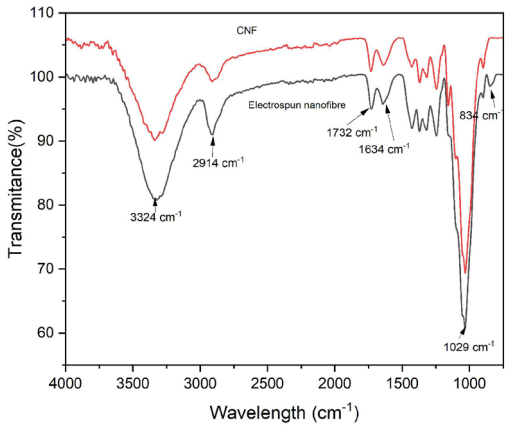

Figure 4. FTIR spectrum for CNF and electrospun nanofiber.

3.3. X-ray Diffraction (XRD) Analysis of Nanocellulose-Based Material

XRD analysis provides essential insights into the crystallographic characteristics of nanocellulose. The deconvoluted data reveal multiple diffraction peaks spanning 2θ values from 5° to 35°. After separating these signals, each spike can now be tied to a particular crystal plane identified by hkl values. This arrangement points to cellulose II or regenerated cellulose structure. Figure 5(a) shows the XRD data of nanofibers incorporating cellulose nanofibrils (CNF), polyvinyl alcohol (PVA), along with Tween 20 (PCT-20). Meanwhile, Figure 5(b) shows another version of this composite that incorporates Tween 80 (PCT-80).

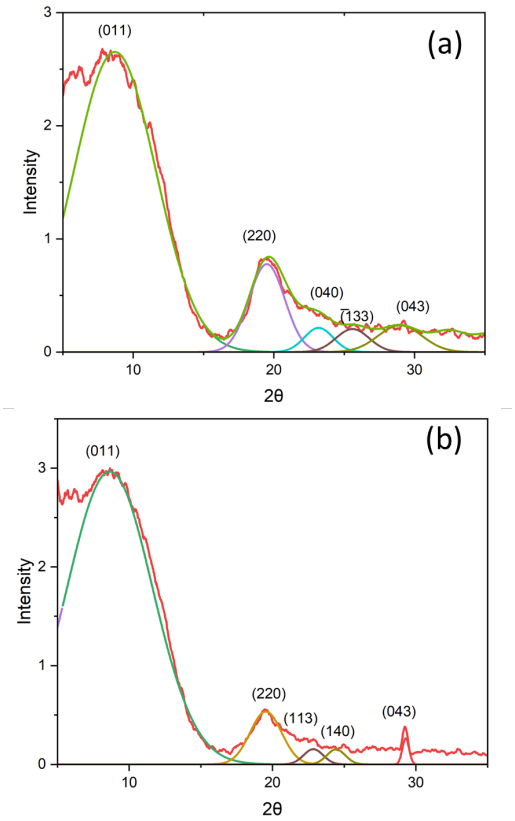

Figure 5. Deconvoluted XRD diagram of (a) PVA-Cellulose-Tween 20 (PCT-20) and (b) PVA-Cellulose-Tween 80 (PCT-80).

Table 1 Comparison between PCT-20 and PCT-80 according to 2θ and their plane numbers

Sample	2θ, (°)	Planes
(a) PCT- 20	7.5, 19.3, 20.9, 23.3, 29.5	(011) (220) (040) (133) (043)
(b) PCT-80	7.5, 19.2, 20.8, 22.4, 29.7	(011) (220) (113) (140) (043)

Figure 5(a) portrays how Tween 80 enhanced crystal ordering better than Tween 20. Molecular arrangement becomes more defined with Tween 80, as evidenced by stronger signals for planes such as (040), (133), and (043). This pattern aligns with what Li, W, and team observed in 2009 for semi-crystalline materials. Look at that image - it shows better separation of peaks, meaning sharper crystalline parts plus a wider hazy patch from Figure 5(b), hinting at more randomness.

3.3.1. Crystallinity Index (CrI)

Using equation [2], the crystallinity index (CrI) was calculated. At 19.3°, the signal reaches its strongest point - this corresponds to the main crystal peak. Meanwhile, down at 16°, the value drops sharply due to a deep trough. According to the standardized intensities, CrI for PCT-20 is 67.9%, compared with 59.3% for PCT-80. This confirms that Tween 20 promotes improved crystallinity, likely due to its longer hydrophobic tail and better compatibility with both CNF and PVA.

The comparison of Figures 5(a) and 5 (b) shows that the (011) and (220) peaks are present in both, but are more intense in the PCT-20 systems. In the meantime, (040) and (133) planes are clearly observed in the PCT-20 composite, suggesting the presence of additional crystalline phases. The planes (113) and (140) in the PCT-80 system exhibit diminished strength and lack of clarity. The wider full width at half maximum (FWHM) observed in Figure 3(b) indicates a smaller crystallite size or an increased amount of amorphous content.

A diffraction pattern suggests the crystalline form of cellulose II, often observed when regenerated cellulose is treated with chemicals such as sodium hydroxide (NaOH). This form is thermodynamically more stable than cellulose I. Its structure fits a monoclinic unit cell that holds the molecules. The slight smearing observed across peaks indicates a reduced crystallite size and suggests more amorphous regions, typical after mechanical stress or spinning methods (Rosa, M. F. et al. 2010).

These findings align with previous morphological images obtained with an FESEM lens and with the clearer crystal structures and fiber continuity observed in the XRD results.

3.4. Field Emission Scanning Electron Microscopy (FESEM)

Figure 6 displays the FESEM micrographs of various electrospun nanofiber formulations, that is, (a) PVA-Cellulose-Tween 20 (PCT-20), (b) PVA-Cellulose-Tween 80 (PCT-80), (c) PVA-Cellulose-Tween 20-semen (PCTS-20), and (d) PVA-Cellulose-Tween 80-semen (PCTS-80).

3.4.1. Fiber Morphology and Uniformity

Figures 6(a) and (b) show smooth and bead-free nanofibers, which lead to more uniform diameter distribution. PCT-80 in Figure 6(b) displays consistently straighter fibers in comparison to PCT-20 depicted in Figure 6(a). This indicates improved interaction and chain alignment of PVA, CNF, and Tween 80 components. This refinement from PCT-20 to PCT 80 likely stems from Tween 80, whose mixed hydrophilic nature can improve polymer blending while stabilizing the spinning jet during the production of electrospun nanofibres.

3.4.2. Effect of Semen Incorporation

The addition of semen in Figure 6(c) and (d) caused some clear changes in the fiber shapes. Figure 6(c) shows the PCTS-20 distorted, fused fibers with pore-like structures. This likely results from interactions between moisture and proteins during fiber formation. In contrast, Figure 6(d), which shows the PCTS-80 sample, although it has some agglomeration, exhibits a relatively fibrous structure. Tween 80, which is in PCTS-80, has higher hydrophobicity and better emulsifying ability. This likely prevents the phases from separating during electrospinning, so the fibers retain their shape better, even with biological material mixed in (Rezaei et al., 2020). Furthermore, matrices with Tween 80 have a denser network and smaller pores, which might help with encapsulation and acting as a barrier (Mahmud et al., 2017).

Nanofibers that remain stable and uniform, such as PCT-80 and PCTS-80, are preferable for biomedical applications, especially those involving encapsulation, including semen preservation. Tween 80 helps distribute the fibers evenly, protect bioactive molecules, and maintain structural integrity during applications and storage.

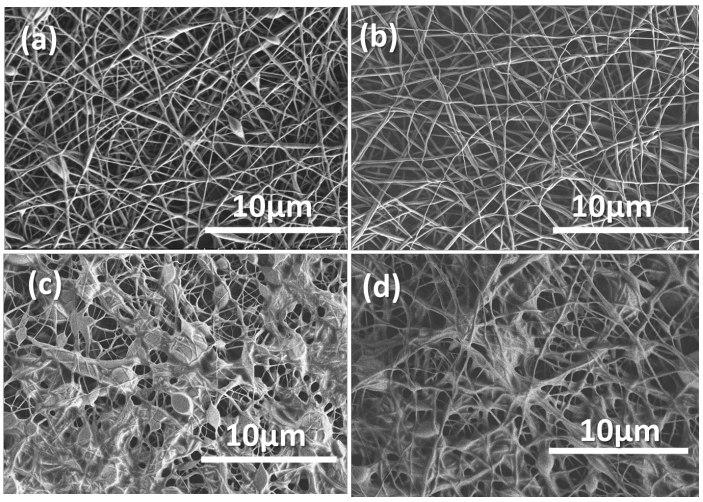

Figure 6. Morphology analysis through FESEM images of (a) PVA-Cellulose-Tween 20 (PCT-20), (b) PVA-Cellulose-Tween 80 (PCT-80), (c) PVA-Cellulose-Tween 20-semen (PCTS-20), (d) PVA-Cellulose-Tween 80-Semen (PCTS-80).

The distribution of fiber length in FESEM images in Figure 6 was then illustrated as histograms with Gaussian fits, as shown in Figure 7.

The PCT20 sample (Figure 7a) has an average fiber length of 3.99 ± 2.09 µm. So, fibers are mostly short, with a moderate spread. Most fibers fall between 2 and 6 µm, but a few go up to 10-14 µm. The distribution is slightly right-skewed, indicating that some longer fibers exist, but most cluster near the average.

The PCT80 sample (Figure 7b) has a longer average fiber length of 5.4 ± 2.1 µm, with a similar spread. The distribution is also right-skewed, with most fibers between 3 and 8 µm, and a few over 12 µm. This shows that PCT80 tends to form longer fibers than PCT20 does.

These differences in fiber length come from the different physical and chemical properties of the two surfactants. Tween 20 has a lower molecular weight and shorter hydrophobic chains than Tween 80. This characteristic is exactly what gives polymer solutions their lower viscosity and surface tension. This helps the fibers endure longer during the electrospinning process. It shortens the fibers and spreads them out more uniformly. Tween 80 has a larger fiber structure and is more hydrophobic, which makes the polymer solution thicker and causes the chains to coil up. This could change how longer fibers are formed by making whipping less unstable and slowing the rate at which the solvent evaporates during electrospinning. The findings of this study are directly proportional to previous studies that stated that the selection of surfactant affects the morphology of nanofibers by modifying the dynamic characteristics of the electrospinning jet (Zhang et al., 2005; Bhardwaj & Kundu, 2010)

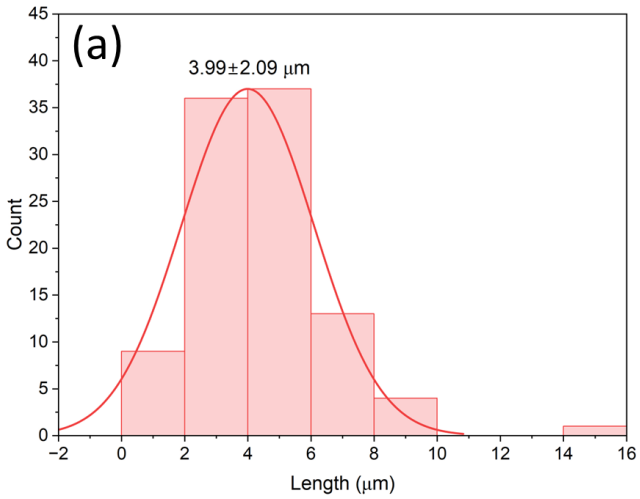

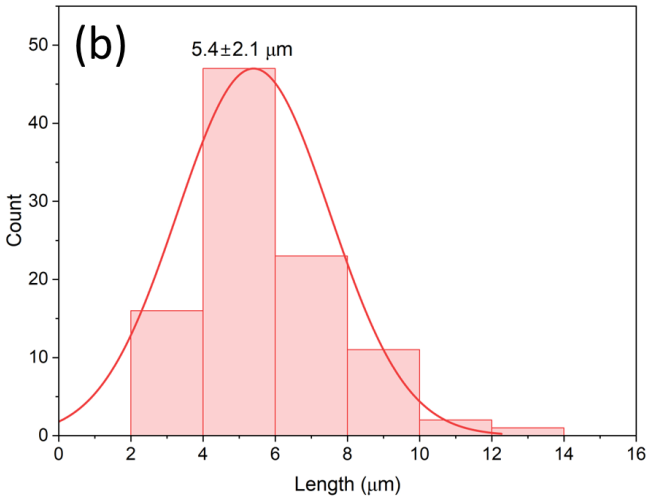

Figure 7. Size distribution histogram with Gaussian fit of (a) PCT-20 and (b) PCT-80.

4. CONCLUSION

The resulting nanocellulose and electrospun materials have been shown to exhibit crystalline and functional chemical characteristics, as evidenced by FTIR and XRD data. For the FTIR spectra, distinct cellulose peaks were found in line with supplementary bands resulting from the addition of polymers and surfactants in the electrospinning method. In the XRD profile, the presence of a semi-crystalline cellulose II structure was demonstrated.

The crystallinity of electrospun nanofibers significantly affects the encapsulation capacity of biomaterials. This is clearly demonstrated by the increase in crystallinity, which indicates denser polymer chains with less free volume, leading to diminished encapsulation efficiency but increased structural stability and prolonged release due to constrained diffusion paths. On the other hand, larger amorphous fibers exhibit increased chain mobility and free volume, thereby increasing encapsulation capacity and often leading to a more rapid release of the encapsulated substance. As a result, a more ideal structure, namely a semi-crystalline one, has the advantage of providing sufficient amorphous domains for the payload. While crystalline portions impede unregulated release. The use of surfactants Tween 20 and Tween 80 can disrupt the crystalline structure and thus increase the efficacy of cellulose-based nanofibers (Zhou et al., 2019; Bhushani & Anandharamakrishnan, 2014; Haider et al., 2018)

Therefore, this structural insight provides a clear picture of the relationship between nanocellulose characteristics and performance in various applications. These include membranes, drug delivery, and packaging. FESEM analysis provides a clear picture of the basic morphology of nanocellulose and electrospun nanofibers. The type of surfactant significantly affects the morphology, with Tween 80 improving fiber uniformity, crystallinity, and structural integrity, particularly for biological encapsulation applications. PVA-CNF-Tween 80 (PCT-80) shows suitable characteristics for bovine semen encapsulation.

ACKNOWLEDGMENTS

The Malaysian Agricultural Research & Development Institute's 12th Malaysian Plan Development Fund has supported this work.

REFERENCE

[1] Bhardwaj, N., & Kundu, S. C. (2010). Electrospinning: A fascinating fiber fabrication technique. *Biotechnology Advances*, 28(3), 325–347.

[2] Bhushani JA, Anandharamakrishnan C. (2014). Electrospinning and electrospraying techniques: Potential food-based applications. *Trends Food Science Technol*ogy, 38(1):21–33.

[3] Chin, N. L., et al. (2018). Extraction and characterization of cellulose from durian rind. *Cellulose Chemistry and Technology*, 52(1-2), 83–89.

[4] French, A. D. (2014). Idealized powder diffraction patterns for cellulose polymorphs. *Cellulose,* 21(2), 885–896.

[5] Haider A, Haider S, Kang IK, Han SS. A (2018) Comprehensive review summarizing the effect of electrospinning parameters and potential applications of nanofibers in biomedical and biotechnology. *Arab J Chem*, 11(8):1165–1188.

[6] Jee, J. P., et al. (2016). Effect of surfactants on the physical properties and release of drug from electrospun nanofibers. *Colloids and Surfaces B: Biointerfaces*, 140, 361–367.

[7] Kargarzadeh, H., Ahmad, I., Abdullah, I., Dufresne, A., Zainudin, S. Y., & Sheltami, R. M. (2012). Cellulose nanocrystal extraction and characterization from kenaf bast fiber. *Cellulose*, 19(3), 855

[8] Li, W., Yue, J., & Liu, S. (2009). Preparation of nanocrystalline cellulose via ultrasound and its reinforcement capability for poly (vinyl alcohol) composites. *Carbohydrate Polymers*, 76(3), 432.

[9] Mahmud, S. et al. (2017). Nanofiber membrane morphology and drug delivery behavior with surfactant modulation. *Materials Science and Engineering:* C, 74, 504–511

[10] Marei, W. F., et al. (2021). Nanotechnology in reproductive medicine: A review of recent advances. *Nanomedicine*, 16(3), 217–235.

[11] Poletto, M., Pistor, V., & Zattera, A. J. (2014). Structural characteristics and thermal properties of native cellulose. *Bioresources*, 9(1), 588-601

[12] Rosa, M. F., Medeiros, E. S., Malmonge, J. A., Gregorski, K. S., Wood, D. F., Mattoso, L. H. C., ... & Orts, W. J. (2010). Cellulose nanowhiskers from coconut husk fibers: Effect of preparation conditions on their thermal and morphological behavior. *Carbohydrate Polymers*, 81(1), 83–92.

[13] Rezaei, A. et al. (2020). Electrospun hybrid nanofibers containing surfactant-stabilized proteins. *ACS Applied Bio Materials*, 3(4), 2664–2675.

[14] Saragusty, J., & Arav, A. (2011). Current progress in oocyte and embryo cryopreservation by slow freezing and vitrification. *Reproduction*, 141(1), 1–19.

[15] Shamsudin, R., et al. (2019). Biocompatibility and biodegradability of cellulose from durian rind. *Polymers,* 11(10), 1683.

[16] Shariatpanahi, M., et al. (2022). Encapsulation of sperm using biomaterials: A promising technique for sperm preservation. *Reproductive Biology and Endocrinology,* 20(1), 24.

[17] Sieme, H., et al. (2016). Sperm preservation in the modern era. *Reproduction in Domestic Animals,* 51(S3), 37–44.

[18] Szyma-Chargot, M., & Zdunek, A. (2013). Use of FT-IR spectra and PCA for the bulk characterization of cell wall residues of fruits and vegetables along a fractionation process. *Food Biophysics*, 8(1), 29-42

[19] Watson, P. F. (2000). The causes of reduced fertility with cryopreserved semen. *Animal Reproduction Science*, 60–61, 481–492.

[20] Widya, R., et al. (2020). Utilization of durian waste for environmental sustainability. *Waste and Biomass Valorization*, 11(5), 2395–2404.

[21] Xie, J., et al. (2008). Electrospun nanofibers for cellular delivery. Nano Today, 3(3–4), 34–43.

[22] Yoon, S. J., et al. (2020). Sperm cryopreservation and its clinical applications. *Clinical and Experimental Reproductive Medicine*, 47(1), 1–7.

[23] Zhang, C., Yuan, X., Wu, L., Han, Y., & Sheng, J. (2005). Study on the morphology of electrospun poly(vinyl alcohol) mats. European Polymer Journal, 41(3), 423–432.

[24] Zhou, Y. et al. (2015). Influence of surfactants on electrospun nanofibers for biomedical applications. Colloids and Surfaces B: *Biointerfaces*, 135, 349–356.

[25] Zhou Y, Yang D, Gao X, Xu Q, Lu F. (2019). Effect of crystallinity of electrospun poly(ε-caprolactone) fibers on encapsulation and release of drugs. *Mater Sci Eng C*, 96:783–791.